Regulated Unmasking of the Cryptic Binding Site for Integrin $\alpha_M\beta_2$ in the γC-Domain of Fibrinogen†

Valeryi K. Lishko,‡ Bohdan Kudryk,§ Valentin P. Yakubenko,‡ Vivien C. Yee,‡ and Tatiana P. Ugarova*,‡

Joseph J. Jacobs Center for Thrombosis and Vascular Biology, Department of Molecular Cardiology, Lerner Research Institute, Cleveland, Ohio 44195, and Lindsley F. Kimball Research Institute, The New York Blood Center, New York, New York 10021

Received June 18, 2002; Revised Manuscript Received August 8, 2002

ABSTRACT: Fibrinogen is a ligand for leukocyte integrin $\alpha_M\beta_2$ (CD11b/CD18, Mac-1) and mediates adhesion and migration of leukocytes during the immune-inflammatory responses. The binding site for $\alpha_M\beta_2$ resides in γC, a constituent subdomain in the D-domain of fibrinogen. The sequence γ383−395 (P2-C) in γC was implicated as the major binding site for $\alpha_M\beta_2$. It is unknown why $\alpha_M\beta_2$ on leukocytes can bind to immobilized fibrinogen in the presence of high concentrations of soluble fibrinogen in plasma. In this study, we have investigated the accessibility of the binding site in fibrinogen for $\alpha_M\beta_2$. We found that the $\alpha_M\beta_2$-binding site in γC is cryptic and identified the mechanism that regulates its unmasking. Proteolytic removal of the small COOH-terminal segment(s) of γC, γ397/405−411, converted the D_{100} fragment of fibrinogen, which contains intact γC and is not able to inhibit adhesion of the $\alpha_M\beta_2$-expressing cells, into the fragment D_{98}, which effectively inhibited cell adhesion. D_{98}, but not D_{100}, bound to the recombinant α_MI-domain, and the α_MI-domain recognition peptide, $\alpha_M(Glu^{253}-Arg^{261})$. Exposure of the P2-C sequence in fibrinogen, D_{100}, and D_{98} was probed with a site-specific mAb. P2-C is not accessible in soluble fibrinogen and D_{100} but becomes exposed in D_{98}. P2-C is also unmasked by immobilization of fibrinogen onto a plastic and by deposition of fibrinogen in the extracellular matrix. Thus, exposure of P2-C by immobilization and by proteolysis correlates with unmasking of the $\alpha_M\beta_2$-binding site in the D-domain. These results demonstrate that conformational alterations regulate the $\alpha_M\beta_2$-binding site in γC and suggest that processes relevant to tissue injury and inflammation are likely to be involved in the activation of the $\alpha_M\beta_2$-binding site in fibrinogen.

The plasma protein fibrinogen (Fg)[1] plays a multifaceted role in extravascular inflammatory responses. Numerous studies using animals with Fg deficiency and afibrinogenemic patients have demonstrated that the manifestation and magnitude of inflammatory responses correlate strongly with the availability of Fg (*1*−*5*). Deposits of Fg and its clotting product, fibrin, were shown at and within the damaged vessel wall under many pathological conditions (*1*, *5*−*9*). Integrin $\alpha_M\beta_2$ (CD11b/CD18, Mac-1) on neutrophils and monocytes serves as a receptor for Fg (*10*, *11*) capable of mediating leukocyte adhesion and migration. Recent characterization of $\alpha_M\beta_2$-deficient mice confirmed that fibrinogen-dependent leukocyte adhesion was diminished in these animals (*12*).

Fibrinogen, a 340 kDa protein, may occur in vivo in two forms: as a soluble plasma protein and as an "immobilized" component of the perivascular matrix after escaping from circulation through leaking vessels. In this latter form, fibrinogen can be deposited either in a proteolytically unaltered form (*6*, *13*) or as a fibrin matrix after activation by thrombin (*6*, *14*).

The binding sites for integrin $\alpha_M\beta_2$ reside in the two peripheral D-domains of the dimeric Fg molecule. Within the D-domain, $\alpha_M\beta_2$ binds to the constituent γC (*15*), a globular domain formed by the COOH-terminal part (143−411) of the γ-chain (*16*, *17*). Two sequences, γ190−202 (designated P1) and γ377−395 (designated P2), in γC were implicated as the putative recognition sites (*18*, *19*). The synthetic peptides P1 and P2 corresponding to these sequences block adhesion of the $\alpha_M\beta_2$-bearing cells and, when immobilized, can directly support cell adhesion (*19*). These peptides are also able to promote a chemotactic migration of the $\alpha_M\beta_2$-expressing cells (*20*). On a molar basis, P2 is a more potent inhibitor of $\alpha_M\beta_2$ function than P1 and is also a more efficient chemotactic agent (*19*, *20*). Within P1, Asp^{199} was shown to be important for the inhibitory activity (*18*). However, when Asp^{199} was mutated to Ala in the recombinant γC-domain, this fragment was as active as its wild-type counterpart in supporting $\alpha_M\beta_2$-mediating adhesion

† This work was supported by NIH Grants HL 63199 and HL 66197, and by the American Heart Association. T.P.U. is an Established Investigator of the American Heart Association.

* To whom correspondence should be addressed at The Cleveland Clinic, Mail Code NB50, 9500 Euclid Ave., Cleveland, OH 44195. E-mail: ugarovt@ccf.org; Tel: (216) 445-8209; FAX: (216) 445-8204.

‡ Lerner Research Institute.

§ The New York Blood Center.

[1] Abbreviations: Fg, human fibrinogen; γC, a globular carboxyl-terminal domain of the γ-chain (γ143−411); α_MI-domain, a region of ~200 amino acids "inserted" in the α-subunit of $\alpha_M\beta_2$; D_{100} and D_{98}, the plasmin fragments of Fg differing in the length of the COOH-termini of the constituent γ-chains; D_s, a fragment obtained by digestion of the D_{100} fragment with stromelysin (MMP-3); MMP, matrix metalloproteinase; mAb, monoclonal antibody; PVP, poly(vinylpyrrolidone); BSA, bovine serum albumin; fMLP, formyl-Met-Leu-Phe; PMA, phorbol-12-myristate-13-acetate; ELISA, enzyme-linked immunosorbent assay; FACS, fluorescence-activated cell sorting; PBS, phosphate-buffered saline; TBS, Tris-buffered saline, HBSS, Hank's balanced salt solution.

10.1021/bi026324c CCC: $22.00
Published on Web 10/04/2002

(*19*). In addition, we have recently demonstrated that mutations of all exposed residues in the P1 segment did not impair the binding function of γC whereas deletion of the P2 sequence resulted in a significant decrease of γC activity.[2] Thus, although the mechanism of the inhibitory activity of the P1 peptide remains to be elucidated, available (*19*, *20*) and our recent data[2] point to P2 as the major binding site in γC for $\alpha_M\beta_2$. The majority of the adhesive-promoting activity in P2 is contained in γ383−395, designated P2-C (*19*). Within $\alpha_M\beta_2$, P2-C binds to the α_MI-domain, a region of ~20 kDa inserted into the α_M subunit (*19*). The binding site for P2-C has been localized to the α_MI-domain segment $Lys^{245}-Arg^{261}$ (*21*).

Previous studies demonstrated that the binding of Fg to neutrophils and monocytes requires prior cell activation with agonists and is governed by a K_d in the micromolar range (*11*, *22*). However, whereas the activation is needed for the binding of soluble Fg, neutrophils, THP-1 monocytoid, and the $\alpha_M\beta_2$-transfected HEK 293 cells readily adhere to immobilized fibrinogen and its derivatives in the absence of receptor activation (*19*, *23*, *24*). Furthermore, the $\alpha_M\beta_2$-mediated adhesive interactions of leukocytes with Fg/fibrin deposits in vivo occur in the presence of high concentrations of soluble Fg such as those that exist in a physiological plasma milieu (~7.5 μM) that should potentially compete for the binding with the receptor. Nevertheless, accumulation of leukocytes at sites of inflammation is not affected by soluble Fg, suggesting that $\alpha_M\beta_2$ can discriminate between the two forms of Fg in favor of protein in the immobilized state. We hypothesized that conformational alteration of Fg occurring upon: (1) its immobilization onto surfaces, including plastic and biomaterials, (2) deposition into the extracellular matrix, and (3) proteolysis may transform it to a ligand competent for recognition by $\alpha_M\beta_2$. In this study, we provide evidence that the $\alpha_M\beta_2$-binding site, and specifically the P2-C sequence, in the γC-domain of Fg is cryptic and identify several biological processes that lead to its unmasking.

EXPERIMENTAL PROCEDURES

Proteins and Peptides. Human Fg was purified from fresh human blood by differential ethanol precipitation (*25*) or obtained from Enzyme Research Laboratories (South Bend, IN). The D_{100} (molecular weight 100 000) fragment was prepared by digestion of Fg with plasmin in the presence of 20 mM $CaCl_2$ and purified as described (*26*). The D_{98} and D_{80} fragments (molecular weights 98 000 and 80 000, respectively) were obtained by digestion of 3−4 mg/mL of the D_{100} fragment with plasmin (Enzyme Research Laboratories, South Bend, IN) at an enzyme:substrate ratio of 1:100 (w/w) in the absence or presence of 5 mM EDTA, respectively, for 20 h at 22 °C. Digestions were terminated by addition of 5 mM diisopropyl fluoride phosphate, 2 mM phenylmethylsulfonyl fluoride, and 250 KIU/mL Trasylol. D_{98} was dialyzed extensively against TBS to remove the low molecular weight peptides generated during proteolysis. D_{80} was purified by gel filtration on Superdex 75. The DD fragment was prepared from cross-linked fibrin as described (*27*). No residual plasmin activity was detected in different D fragment preparations, as evaluated by using a specific substrate, S-2251 (DiaPharma, Franklin, OH). The D_s fragment was obtained by digestion of D_{100} with stromelysin (MMP-3) in TBS in the presence of 5 mM $CaCl_2$ at a 1:100 enzyme:substrate ratio for 21 h at 22 °C. Digestion was terminated with 10 mM EDTA. Fg and fragments were biotinylated with EZ-link Sulfo-NHS-LC-Biotin (Pierce) according to the manufacturer's protocol or labeled with ^{125}I by the Chloramine T procedure. The production and purification of the recombinant α_MI-domain were described in (*21*). P2 and P2-C, peptides corresponding to Fg sequences γ377−395 and γ383−395, respectively, and the α_MI-domain peptide $\alpha_M(Glu^{253}-Arg^{261})$ were synthesized and purified as described (*19*, *21*). In addition, peptides corresponding to fibrinogen sequences $\gamma Leu^{392}-Val^{411}$, $\gamma Leu^{392}-His^{400}$ were synthesized. The γ385−411 fragment was purified from CNBr-cleaved Fg and isolated by HPLC. The γ392−406 was isolated from the trypsin digest of γ385−411 and purified by HPLC.

Cells. The $\alpha_M\beta_2$-expressing HEK 293 cells (*28*) were maintained in DMEM/F-12 (BioWhittaker, Walkersville, MD) supplemented with 10% fetal bovine serum, 25 mM HEPES, and antibiotics. WI38 human lung fibroblasts were obtained from American Type Culture Collection (Rockville, MD) and were grown in DMEM-F12 media supplemented with 10% FBS and 2 mM sodium pyruvate.

Neutrophils were isolated under sterile conditions from human peripheral blood obtained from consenting volunteers and anticoagulated with acid−citrate−dextrose. Isolation was performed by using density centrifugation on Ficoll-Hypaque (Amersham Pharmacia Biotech), followed by dextran sedimentation of erythrocytes and hypotonic lysis of residual erythrocytes.

Monoclonal Antibodies. The mAb 4-2 (referred to also as "anti-P2-C" in the present study) was produced using a mixture of chains derived from cross-linked human fibrin as immunogen (*29*). Mab 4-2 was IgG1,κ isotype. The epitope recognized by mAb 4-2 was characterized using synthetic peptides and peptides derived from Fg digests. In competition ELISA experiments, synthetic peptide γ392−411 was a strong inhibitor of mAb binding to immobilized Fg (IC_{50} = 0.36 μM). The antibody also reacts fully with γ392−406 and γ392−400. It showed no reactivity with a γ397−411. That a part of the epitope for mAb 4-2 may reside in the NH_2-terminal part of γ392−400 is supported by the data that the antibody reacted weakly with the P2 peptide (γ377−395) and its derivative P2-C (γ383−395) in ELISA, and it also inhibited adhesion of the $\alpha_M\beta_2$-expressing cells to immobilized P2-C (*19*).

MAb 8A11 directed against human fibronection and mAb 2G5 recognizing the epitope at γ373−385 of human Fg were described previously (*30*, *31*). MAb 4A5 against γ406−411 (*32*) was provided by Dr. G. Matsueda (Bristol-Meyers Squibb).

Adhesion Assays. Adhesion assays with neutrophils were performed as described (*33*). Briefly, neutrophils in HBSS supplemented with 0.1% BSA were labeled with Calcein AM (Molecular Probes, Eugene, OR) for 30 min at 37 °C. Neutrophils at a concentration 5×10^6 cells/mL were activated with 10 nM PMA or 100 nM fMLP, and aliquots (100 μL) were added to the wells of 96-well microtiter plates

[2] Merkulov, S., Lishko,V., Podolnikova, N., et al., manuscript in preparation.

(Immulon 4 HBX, Dynex Technologies, Chantilly, VA) coated with different ligands. For inhibition experiments, neutrophils activated with agonists for 5 min at 22 °C or unstimulated cells were mixed with either D_{100} or D_{98} fragments for 20 min at 22 °C before they were added to the coated wells. After 30 min of incubation at 37 °C in 5% CO_2, the nonadherent cells were removed by two gentle washes with PBS. Fluorescence was measured in a fluorescence plate reader (Applied Biosystems, Framingham, MA), and the number of adherent cells was determined from a standard curve.

Adhesion assays with the $\alpha_M\beta_2$-expressing cells were performed essentially as described (*19*). Briefly, the 48 well tissue culture plates (Costar, Cambridge, MA) were coated with 10 μg/mL of the D_{100} and D_{98} fragments or 5−10 μg/mL of the P2-C peptide for 3h at 37 °C. The coated wells were post-coated with 0.5% PVP for 1 h at 22 °C. The harvested cells were washed in HBSS/HEPES solution and were labeled with $Na_2{}^{51}CrO_4$ (0.5 mCi/mL) for 30 min at 22 °C. After being washed, the cells were resuspended at 5×10^5/mL in HBSS/HEPES supplemented with 1 mM Ca^{2+}, 1 mM Mg^{2+}, and 10 mg/mL BSA. Aliquots (100 μL) of the labeled cells were added to the wells and incubated for 25 min at 37 °C in a 5% CO_2 humidified atmosphere. The nonadherent cells were removed by three washes with PBS, and adherent cells were solubilized with 2% SDS. ^{51}Cr was quantitated in a β counter. For inhibition experiments, the cells were mixed with different amounts of Fg, D_{100}, and D_{98} fragments and then incubated for 15 min at 22 °C with gentle shaking before addition to the wells coated with the D_{100} fragment or P2-C. Fg, purified by differential ethanol precipitation (*25*), was used for inhibition experiments.

Competitive Inhibition ELISA. For solid-phase immunoassays, polystyrene microtiter plates (Titertek, ICN Pharmaceuticals, Costa Mesa, CA) were coated with 0.5 μg/mL of the D_{100} fragment for 3 h at 37 °C or overnight at 4 °C. The wells were post-coated with 1% BSA for 1 h at 22 °C and then washed with PBS + 0.05% Tween 20; 0.5−1 μg/mL mAb 4-2 (final concentrations of mAb) was mixed with various amounts of Fg, D_{100}, D_{98}, DD, or D_{80} fragments in PBS + 100 KIU/mL Trasylol, and 100 μL aliquots were added to wells. After incubation for 1.5 h at 37 °C, the plates were washed, and goat anti-mouse IgG, conjugated to alkaline phosphatase, was added. Mab binding was detected by reaction with *p*-nitrophenyl phosphate.

Solid-Phase Binding Assays. Plates (96 well; Immulon 2 HB, Dynex Technologies Inc., Chantilly, VA) were coated with 100 μM $\alpha_M(Glu^{253}-Arg^{261})$ peptide in PBS or with 10 μg/mL of the recombinant α_MI-domain in TBS supplemented with 1 mM Ca^{2+} and 1 mM Mg^{2+} overnight at 4 °C. Biotinylated D_{100} and D_{98} fragments in TBS, containing 1 mM Ca^{2+}, 1 mM Mg^{2+}, 100 KIU/mL Trasylol, and 0.05% Tween 20, were added to wells coated with the α_MI-domain peptides or the recombinant α_MI-domain and incubated for 2.5 h at 37 °C. After the wells were washed, streptavidin conjugated to alkaline phosphatase (Pierce) was added and incubated for 45 min at 37 °C. The binding of fragments was detected by reaction with *p*-nitrophenyl phosphate, measuring the absorbance at 405 nm.

Immunofluorescent Studies. The extracellular matrix deposited by WI38 human lung fibroblasts was analyzed by immunofluorescent staining. Cells were trypsinized and cultured on glass coverslips in 12-well plates in DMEM-F12 supplemented with 10% FBS and 2 mM sodium pyruvate for 72 h. Cells were rinsed, and the fresh medium supplemented with 0.1−0.25 mg/mL human Fg was added. After 24 h, a thin film of fibrin formed on the top of the fibroblast's layer was removed, the coverslips were washed in 1.0 mL of PBS, and the cells were fixed in 3.7% paraformaldehyde for 30 min. Wells were blocked with 3% normal goat serum in PBS (blocking buffer) for 1 h after which primary mAbs directed against human fibronectin and Fg diluted in the blocking buffer were added. After 2 h incubation, the slides were washed with TBS + 0.05% Tween-20, and the secondary goat anti-mouse IgG conjugated to Alexa 488 (1:1000 dilution) was added for 30 min. Images of the fluorescent-labeled extracellular matrix were obtained using a Leica TCS-NT laser scanning confocal microscope (Leica, Heidelberg, Germany).

Analytical Procedures. The D_{100} and D_{98} fragments were analyzed by Western blot analyses with mAbs 4-2 and 4A5. For these analyses, the samples under reducing conditions were separated by 11% SDS−PAGE in a Laemmli buffer system and transferred onto Immobilon-P membranes (Millipore) which were then incubated with selected mAbs. Bound mAbs were detected by reaction with a peroxidase-conjugated secondary antibody (Bio-Rad) followed by addition of the substrate 4-chloro-1-naphthol.

To determine the amount of Fg and fragments immobilized onto the wells of the plates, various amounts of radiolabeled Fg, D_{100}, and D_{98} were adsorbed onto the plastic for 3 h at 37 °C, post-coated with PVP, and then washed with PBS. Bound proteins were solubilized in 2% SDS + 0.5 N NaOH, and the released radioactivity was quantitated in a γ counter. The amount of the protein bound to the wells was calculated on the basis of the amount of radioactivity recovered and the specific activity of ^{125}I-D_{100} and ^{125}I-D_{98}.

For amino acid sequence analysis, the constituent chains of the D_{80} fragment were separated by SDS−PAGE after reduction with β-mercaptoethanol, the band corresponding to the γ-chain was excised, and the NH_2-terminus of the protein was determined by direct sequencing for 10 cycles.

RESULTS

Effect of the D_{100} Fragment on Adhesion of the $\alpha_M\beta_2$-Bearing Cells to Fg and Its Derivatives. Previous studies have demonstrated that stimulated neutrophils adhere to Fg and fibrin both in vitro and in vivo and that this interaction is mediated by integrins $\alpha_M\beta_2$ and $\alpha_X\beta_2$ (*12*, *23*, *24*), with $\alpha_M\beta_2$ playing a principal role. The $\alpha_M\beta_2$-mediated adhesive interactions of neutrophils occur in plasma that contains 2−4 mg of Fg/mL. Therefore, we have examined the effect of soluble D_{100} fragment, in which the binding site for $\alpha_M\beta_2$ resides, on adhesion of activated and unstimulated neutrophils. In confirmation of previous findings (*23*, *24*), unstimulated neutrophils adhered to Fg and D_{100} (Figure 1A). Stimulation of neutrophils with fMLP and PMA enhanced adhesion ∼2- and ∼3.5-fold, respectively (Figure 1A). Adhesion of neutrophils was $\alpha_M\beta_2$-dependent since saturating concentrations (20−40 μg/mL) of mAbs 44a and IB4 directed against α_M and β_2 integrin subunits, respectively, blocked adhesion by 80−90% (not shown). However, adhesion of either stimulated or unstimulated neutrophils to

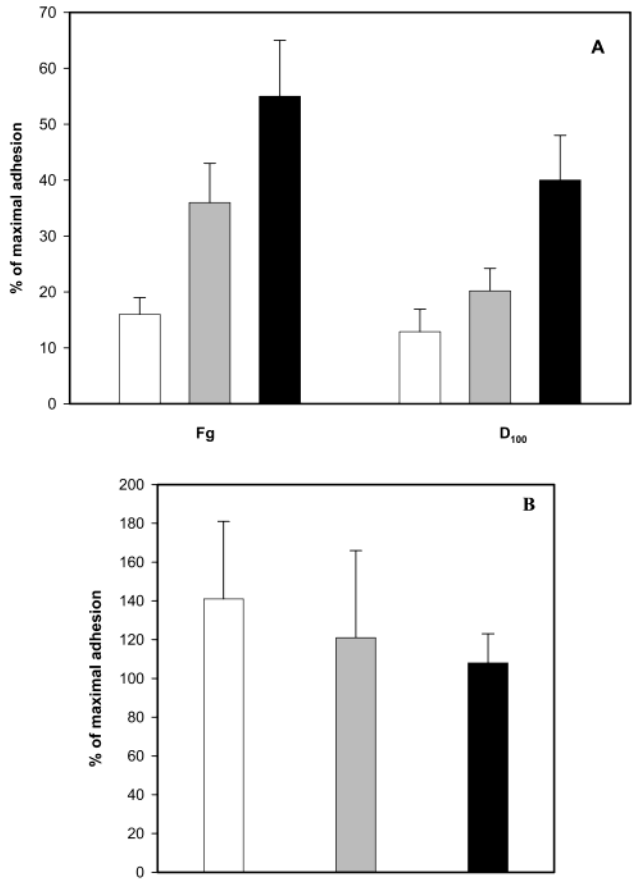

FIGURE 1: Effect of the D_{100} fragment on adhesion of neutrophils to Fg and D_{100}. (A) Neutrophils were isolated from human blood, resuspended in HBSS+0.1% BSA, and labeled with calcein. Cells were suspended at 5×10^6/mL in the absence (open bars) or in the presence of activators, 100 nM fMLP (gray bars) and 10 nM PMA (black bars). After 5 min incubation at 22 °C, aliquots of cells (100 μL) were added to the wells coated with 2.5 μg/mL Fg or D_{100}. After 25 min at 37 °C, nonadherent cells were removed, and fluorescence of adherent cells was measured. Data are expressed as a percentage of added cells. (B) Effect of D_{100} on adhesion of unstimulated (open bars), fMLP-activated (gray bars), and PMA-activated (black bars) neutrophils. Unstimulated or agonist-stimulated neutrophils were preincubated with 3.0 mg/mL (final concentration) D_{100} for 20 min at 22 °C, and then aliquots (5×10^5) of cells were added to the wells coated with 2.5 μg/mL D_{100}. The amount of D_{100} immobilized onto the plastic surface was quantitated using ^{125}I-D_{100}. At an input concentration of 2.5 μg/mL (0.1 mL/well), 0.112 μg of protein was bound. Data are expressed as a percentage of control (adhesion in the absence of added proteins). Results are the mean ± SE values from 6−8 individual experiments performed with quadruplicates at each experimental point.

Fg or to D_{100} was not affected by soluble D_{100} at 3.0 mg/mL, i.e., at ~2700-fold excess over the immobilized ligand (Figure 1B, adhesion to D_{100} is shown). Also in previous studies, 3 mg/mL soluble Fg produced only 25% inhibition of adhesion of TNFα-stimulated neutrophils to Fg-coated surfaces (*24*). Thus, these data indicated that soluble D_{100} was not an efficient inhibitor of adhesion of neutrophils to immobilized D_{100}.

Since neutrophils are known to express several integrins that can bind Fg, we have performed inhibition analyses with soluble Fg and D_{100} using the $\alpha_M\beta_2$-expressing HEK 293 cells. We have shown previously that these cells bind Fg and its derivatives, including the fragment D_{100}, recombinant γC-domain, and the P2-C peptide, specifically through $\alpha_M\beta_2$ (*15*, *19*, *33*, *34*). However, while immobilized D_{100} and Fg supported efficient adhesion, soluble intact proteins were poor inhibitors of $\alpha_M\beta_2$-mediated cell adhesion to immobilized D_{100} fragment or P2-C peptide (Figure 2A,B). No inhibition was produced by soluble Fg at 30 μM, i.e., at a (4.05×10^3)-fold molar excess of soluble protein to the immobilized D_{100} (Figure 2A). The D_{100} produced little inhibition (~10%) at 30 μM, the maximal testable concentration. The D_{100} fragment also did not inhibit cell adhesion to immobilized P2-C (Figure 2B). Furthermore, in parallel experiments we attempted to determine the affinity of Fg and D_{100} for $\alpha_M\beta_2$ by measuring binding of ^{125}I-Fg and ^{125}I-D_{100} to the $\alpha_M\beta_2$-expressing cells. Specific binding was not detected, indicating that the affinity was low. Since cells adhered to immobilized proteins but did not interact with soluble ligands, these results suggested that the $\alpha_M\beta_2$-binding site might not be available in soluble Fg and D_{100} but becomes unmasked in the immobilized ligands. Therefore, we sought to determine the processes that regulate unmasking of the $\alpha_M\beta_2$-binding site in Fg and D_{100}. The initial insight into the possible mechanism of exposure of the $\alpha_M\beta_2$-binding site in Fg was obtained in the experiments with a proteolytically modified form of D_{100}. When D_{100} was subjected to further digestion with plasmin in the absence or in the presence of 5 mM EDTA to produce the fragments with molecular masses of 98 and 80 kDa, respectively, these latter fragments were effective inhibitors of adhesion (Figure 2A,B; shown for D_{98}). As shown in Figure 2C, D_{98} also efficiently inhibited adhesion of activated neutrophils to the immobilized D_{100}. The capacity of the immobilized D_{98} fragment to directly support adhesion of the $\alpha_M\beta_2$-expressing cells was then tested. As shown in Figure 3, the adhesion-promoting activity of D_{98} was comparable to that of D_{100}, and the cells appeared similar on both substrates (not shown). Thus, although the $\alpha_M\beta_2$-expressing cells efficiently adhered to immobilized D_{100} fragment and to Fg, they did not bind Fg and D_{100} in solution. In contrast, immobilized D_{98} supported adhesion and was an efficient inhibitor of adhesion when in solution, suggesting that a proteolytic alteration unmasked receptor recognition site(s).

Characterization of the D_{98} Fragment of Fg. The D_{98} fragment was characterized further. Comparison of D_{100} and D_{98} by SDS−PAGE under reducing conditions demonstrated that the γ-chain of D_{98} migrated slightly faster than the constituent γ-chain of D_{100} (Figure 4A, lanes 2 and 1) while the mobility of the β-chain did not change. It is well documented that, depending on the stage of Fg digestion with plasmin, the generated D_{100} fragment may contain two γ-chain variants differing by the NH_2-termini (*35*, *36*). The early D_{100} fragment contains γ63−411 (referred to as γ_{1A}), and the late D_{100} fragment contains γ86−411 (referred to as γ_1). These two variants are seen as a doublet in our D_{100} (Figure 4A, lanes 1, 4, and schematically shown in Figure 4C). Complete transformation of γ_{1A} to γ_1 occurs upon prolonged digestion of D_{100} by plasmin in the presence of 5 mM Ca^{2+} (*36*). We have found that transition of the γ_{1A} to γ_1 did not augment the capability of the D_{100} fragment to inhibit cell adhesion (not shown). Therefore, removal of γ63−85 seems not to be responsible for the inhibitory potency of D_{98}. The D_{100} and D_{98} fragments were analyzed further by Western blot analysis with two mAbs specific for

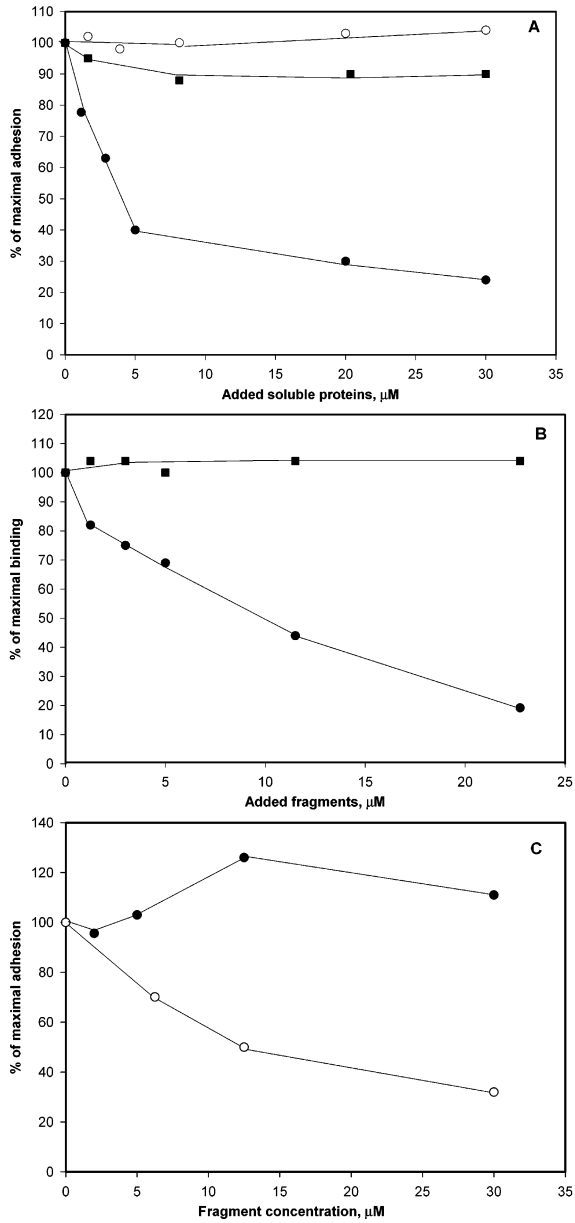

FIGURE 2: Effect of Fg, D_{100}, and D_{98} fragments on adhesion of the $\alpha_M\beta_2$-expressing HEK 293 cells and neutrophils. ^{51}Cr-labeled $\alpha_M\beta_2$-transfected cells in HBSS/HEPES supplemented with 1 mM Ca^{2+}, 1 mM Mg^{2+}, and 1% BSA (adhesion buffer) were incubated with increasing concentrations of Fg (○), D_{100} (■), and D_{98} (●) for 15 min at 22 °C with constant agitation. The proteins were dialyzed against adhesion buffer for 6−20 h prior to the experiment. Aliquots (5×10^4 cells/0.1 mL) were added to microtiter wells coated with 10 μg/mL D_{100} fragment (A) or 10 μg/mL P2-C peptide (B) and post-coated with 0.5% PVP. After 25 min at 37 °C in a humidified atmosphere containing 5% CO_2, the nonadherent cells were removed by three washes with PBS, the adherent cells were solubilized with 2% SDS, and their radioactivity was counted in a β-counter. Data are expressed as a percentage of control (adhesion in the absence of competing proteins) and are the mean ± SE of 3−6 individual experiments performed with triplicate determinations in each experiment. (C) Adhesion of fMLP-activated neutrophils in the presence of the D_{100} (●) or D_{98} (○) fragments. Neutrophils activated with 100 nM fMLP were preincubated with different concentrations of D_{100} or D_{98} for 20 min and then added to the wells coated with 2.5 μg/mL D_{100}. Adhesion was done as described under Experimental Procedures. The molecular weight of Fg was assumed to be 170 000 as each subunit of the dimeric Fg contains one D domain. The amount of D_{100} immobilized onto the plastic surface was quantitated using ^{125}I-D_{100}. At an input concentration of 10 μg/mL (0.1 mL/well), 0.125 μg of protein was bound.

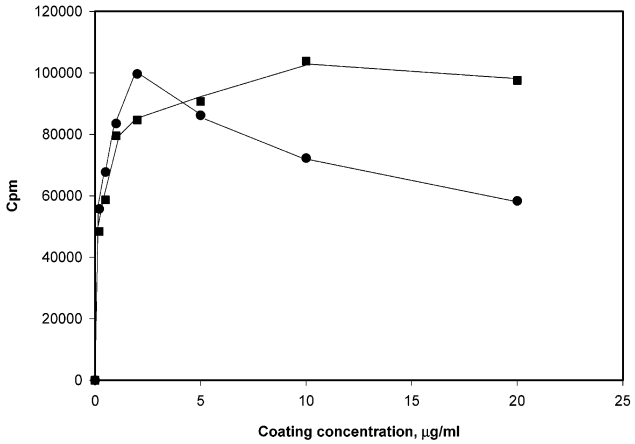

FIGURE 3: Adhesion of the $\alpha_M\beta_2$-expressing cells to the immobilized D_{100} and D_{98} fragments. Aliquots (0.1 mL) of ^{51}Cr-labeled cells (5×10^4) in DMEM/F-12 supplemented with 1 mM Ca^{2+}, 1 mM Mg^{2+}, and 1% BSA were added to wells coated with different concentrations of D_{100} (■) and D_{98} (●). After 25 min at 37 °C, the nonadherent cells were removed, and adherent cells were solubilized to count the bound radioactivity. Data are expressed as cpm of adherent cells.

the COOH-terminus of the γ-chain. MAb 4-2 recognizes the epitope(s) residing within γ392−400, and mAb 4A5 recognizes an epitope in the extreme COOH-terminus of the γ-chain at γ406−411 (*32*). The bands corresponding to the γ-chains in D_{100} (Figure 4B, lane 3) and a band corresponding to the γ-chain in D_{98} (denoted $\gamma_{1\Delta C}$, Figure 4B, lane 2) reacted with mAb 4-2, consistent with the epitope(s) within γ392−400 being preserved in both fragments. MAb 4A5 bound only to D_{100} which contains the unaltered COOH-termini of the γ-chains and did not react with D_{98} (Figure 4B, lanes 6 and 5, respectively). Thus, the COOH-terminal part of the γ-chain in D_{98} was removed.

Exposure of the P2-C Sequence in Fg and Its Proteolytic Fragments. Since the P2-C sequence was implicated as the major $\alpha_M\beta_2$-binding site (*19*),[2] we probed its exposure in Fg, D_{100}, and D_{98}, either in soluble or in immobilized states, using the site-specific mAb 4-2 directed against γ392−400. Since mAb 4-2 reacted with the γ383−395 peptide (P2-C), it suggested that the NH_2-terminal region of γ392−400 may contain part of the epitope (*19*). Furthermore, we have previously demonstrated that mAb 4-2 inhibited adhesion of the $\alpha_M\beta_2$-expressing cells to immobilized D_{100} (*19*), indicating that the mAb could be an effective reporter of changes in the conformational status of the P2-C region of the γ-chain in different Fg derivatives.

The interaction of mAbs with soluble Fg and its plasmin fragments was tested using a competitive ELISA format. MAb 4-2 strongly interacted with immobilized Fg and D_{100} in a saturable and dose-dependent manner. At 0.5 μg/mL coating concentration of D_{100} and subsaturating concentration of the antibody (0.5 μg/mL), the signal at 405 nm in ELISA was typically 2.5−3.0 after 40 min at 37 °C. When used as a competitor, soluble Fg was a poor inhibitor of antibody binding. As shown in Figure 5A, at 20 μM, i.e., at (6.7×10^3)-fold molar excess of soluble Fg to the mAb [($\sim 1.5 \times 10^4$)-fold excess of soluble over immobilized ligand], it inhibited about 20% of mAb 4-2 binding to immobilized D_{100}. The D_{100} fragment was also a weak inhibitor of antibody binding to surface-bound protein. 50% inhibition was

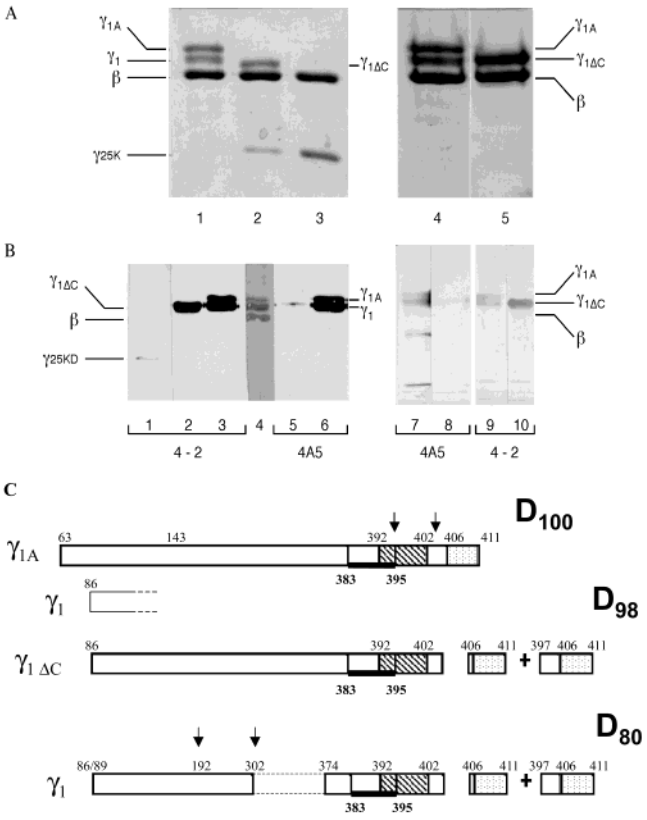

FIGURE 4: Polypeptide chain composition of the D_{100}, D_{98}, D_{80}, and D_S fragments. (A) SDS−PAGE analysis of component chains of D_{100} (lanes 1 and 4), D_{98} (lane 2), D_{80} (lane 3), and D_S (lane 5) fragments of Fg. Digestions with plasmin or stromelysin to generate the D_{98}, D_{80}, and D_S fragments, respectively, were performed as described under Experimental Procedures. Positions of γ_{1A}, γ_1, and β chains in D_{100}; and $\gamma_{1\Delta C}$ in D_{98} and D_s are shown. γ25K is the γ-chain remnant with molecular mass 25 kDa in D_{80}. (B) Proteins were reduced with 2% β-mercaptoethanol, electrophoresed on 11% SDS−PAGE, transferred to Immobilon-P membranes, and probed with mAb 4A5 (1:1500 dilution of ascites) or mAb 4-2 (2 μg/mL affinity-purified IgG). D_{100}: lanes 3, 6, 7, and 9; D_{98}: lanes 2 and 5; D_S: lanes 8 and 10; D_{80}: lane 1 (note that segment γ374−405 [or γ374−396] noncovalently inserted in D_{80} dissociates from γC under SDS conditions). Lane 4 shows D_{100} stained by Coomassie blue. (C) Schematic representation of functional sites and suggested cleavage sites in the γ-chains of D_{100}, D_{98}, and D_{80} fragments. D_{100} contains two populations of γ-chains, γ_{1A} and γ_1. The positions of epitopes for mAb 4A5 (γ406−411) and 4-2 (γ392−402) are shown as dotted and striped boxes, respectively. The solid bar between γ383 and γ395 represents P2-C. Numbers indicate positions of amino acid residues in the γ-chain and are not to a scale. γ143 indicates the NH_2-terminus of γC. The COOH-terminal segments γ405/406−411 and γ397−411 are removed by proteolysis in D_{98}. The segment γ374−405 (and/or γ374−396) is noncovalently inserted (dashed lines) within γC in the D_{80} fragment (*41*). The short arrows indicate plasmin cleavage sites. Direct sequencing of the constituent γ-chain in our D_{80} demonstrated that ~10−15% of the molecules contained ^{193}VFQKRLDG^{200} as the NH_2-terminus, consistent with previous findings (*43*).

produced at 15.8 ± 2.2 μM (Figure 5A). Poor inhibition of mAb binding is consistent with inaccessibility of the P2-C epitope in intact soluble Fg and in the D_{100} fragment. In contrast, D_{98} and D_{80} inhibited the binding of mAb 4-2 to immobilized D_{100} efficiently and in a dose-dependent manner, with D_{80} being the more efficient inhibitor; 50% inhibition of antibody binding was achieved at 2.7 ± 0.7 μM and 1.8 ± 0.2 μM D_{98} and D_{80}, respectively. In addition, the DD-fragment, obtained from the cross-linked fibrin by plasmin,

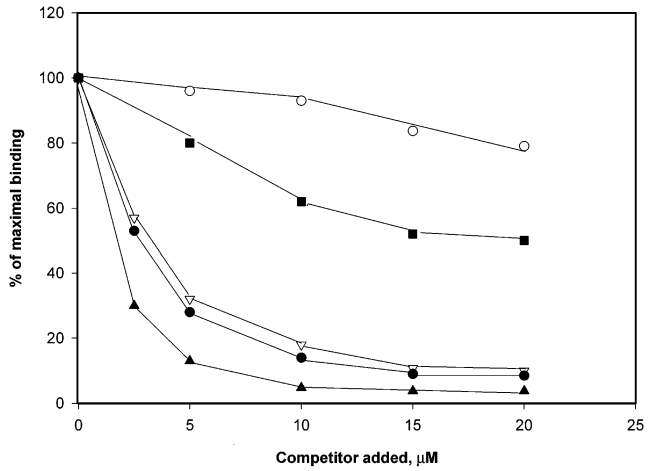

FIGURE 5: Immunochemical characterization of exposure of the P2-C sequence in soluble Fg and its plasmin fragments. Inhibition of mAb 4-2 binding to surface-bound D_{100} by soluble Fg and the D_{100}, D_{98}, D_{80}, and DD fragments. Increasing concentrations of Fg (○), D_{100} (■), D_{98} (●), D_{80} (▲), and DD (▽) fragments were mixed with 0.5 μg/mL mAb 4-2 (final concentration), and 0.1 mL aliquots were added to the wells coated with 0.5 μg/mL D_{100} and post-coated with 1% BSA. After 1.5 h at 37 °C, wells were washed with PBS+0.05% Tween 20, and the second antibody (conjugated with alkaline phosphatase) was added for 1 h at 37 °C. Antibody binding was detected by reaction with *p*-nitrophenyl phosphate, and absorbance at 405 nm was measured. The amount of protein adsorbed on the plastic was determined using radiolabeled D_{100} as described under Experimental Procedures. At the input concentration of 0.5 μg/mL (0.1 mL), 0.023 μg of added D_{100} was bound. Data are expressed as percent of maximal binding of the mAbs in the absence of competitors.

also inhibited the binding of mAb 4-2 to immobilized D_{100}, and its inhibitory effect was similar to that of D_{98}; 50% inhibition was achieved at 3 ± 0.15 μM DD.

A fragment similar to D_{98} was obtained by digesting D_{100} with stromelysin (MMP-3) which cleaves the γ-chain at γ404−405 (*37*). The state of the γ-chain in this fragment (designated D_s) as analyzed by SDS−PAGE and by Western blotting with site-specific antibodies is shown in Figure 4A,B. The COOH-terminus of D_s was degraded as evidenced by SDS−PAGE (Figure 4A, lane 5) and by the lack of immunoreactivity with mAb 4A5 (Figure 4B, lane 8). At the same time, the epitopes within γ392−400 were preserved as demonstrated by staining with mAb 4-2 (Figure 4B, lane 10). When tested in a competitive ELISA, D_s was a more potent inhibitor of mAb 4-2 binding than D_{100}: at 10 μM, D_s produced 61 ± 6% inhibition compared to 30 ± 6% by D_{100}. However, D_s was less active than D_{98} and D_{80} fragments which at 10 μM each produced 87% and 95% inhibition, respectively.

Thus, the above results indicated that P2-C is poorly exposed in soluble Fg and its proteolytic fragment D_{100} but become unmasked in the immobilized states of these molecules. Furthermore, this epitope is unmasked by proteolysis with proteases that cleave the COOH-terminus of the γ-chain.

Binding of D_{98} and D_{100} Fragments to the Recombinant I-Domain and the α_MI-Domain Recognition Peptides. It is known that the α_MI-domain of $\alpha_M\beta_2$ is responsible for recognition of the P2-C sequence (*19*). To further substantiate the role of the COOH-terminal part of the γ-chain in regulating exposure of the $\alpha_M\beta_2$-binding site, we compared

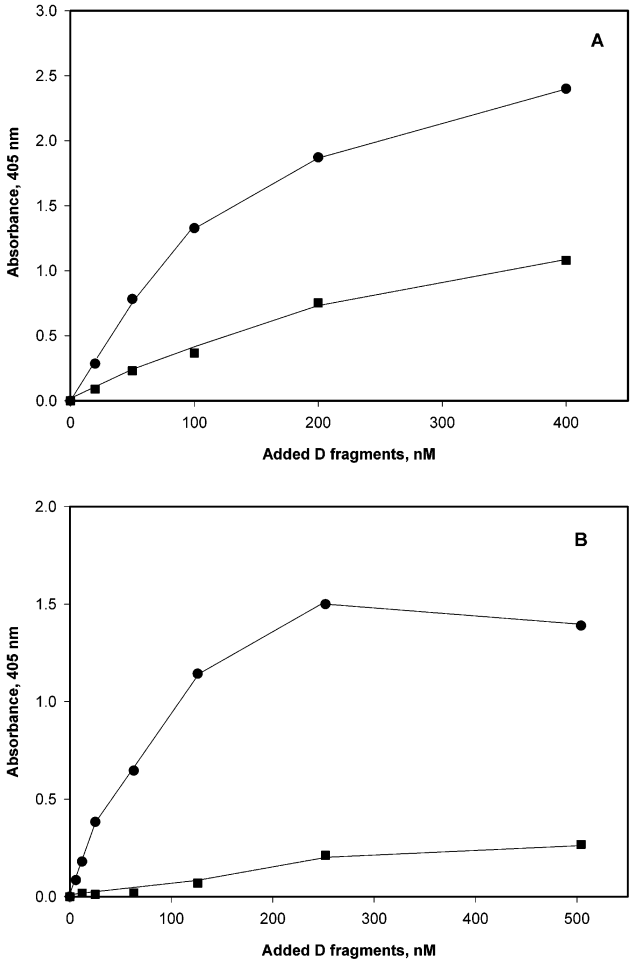

FIGURE 6: Binding of the D_{100} and D_{98} fragments to the α_MI-domain and to the α_MI-domain recognition peptide. (A) Different concentrations of biotinylated D_{100} (■) and D_{98} (●) fragments in 0.05 M TBS, supplemented with 1 mM Ca^{2+}, 1 mM Mg^{2+}, 200 KIU/mL Trasylol, and 0.05% Tween 20, were added to the wells coated with 10 μg/mL of the recombinant α_MI-domain, and incubated for 3 h at 37 °C. After washing, the bound fragments were detected using streptavidin conjugated to alkaline phosphatase, with *p*-nitrophenyl phosphate for disclosure. Nonspecific binding to BSA-coated wells was subtracted. (B) The microtiter plates were coated with 100 μM $\alpha_M(Glu^{253}-Arg^{261})$ overnight at 4 °C and post-coated with 3% BSA. Then different concentrations of biotinylated D_{100} (■) and D_{98} (●) fragments in PBS+0.05% Tween 20 were added to the wells for 3 h at 37 °C. After washing, bound fragments were detected as above.

the binding of the D_{98} and D_{100} fragments to the recombinant α_MI-domain. Previous data demonstrated that the D_{98} fragment specifically bound to the immobilized α_MI-domain and P2-C inhibited this interaction (*21*). As shown in Figure 6A, biotinylated D_{98} bound to the immobilized α_MI-domain at higher levels than biotinylated D_{100}. Furthermore, additional experiments confirmed that D_{98} had a higher affinity for the α_MI-domain than D_{100}. We have previously found that within the α_MI-domain, P2-C binds to two adjacent sequences, $\alpha_M(Lys^{245}-Tyr^{252})$ and $\alpha_M(Glu^{253}-Arg^{261})$ (*21*). Therefore, we have compared the binding of biotinylated D_{100} and D_{98} to the immobilized peptide $\alpha_M(Glu^{253}-Arg^{261})$. As shown in Figure 6B, only D_{98} bound to $\alpha_M(Glu^{253}-Arg^{261})$ while D_{100} did not interact. These results are consistent with exposure of the $\alpha_M\beta_2$-binding site in the D_{98} fragment.

Deposition of Fg into the Extracellular Matrix Results in Unmasking of the P2-C Sequence. It has been shown that

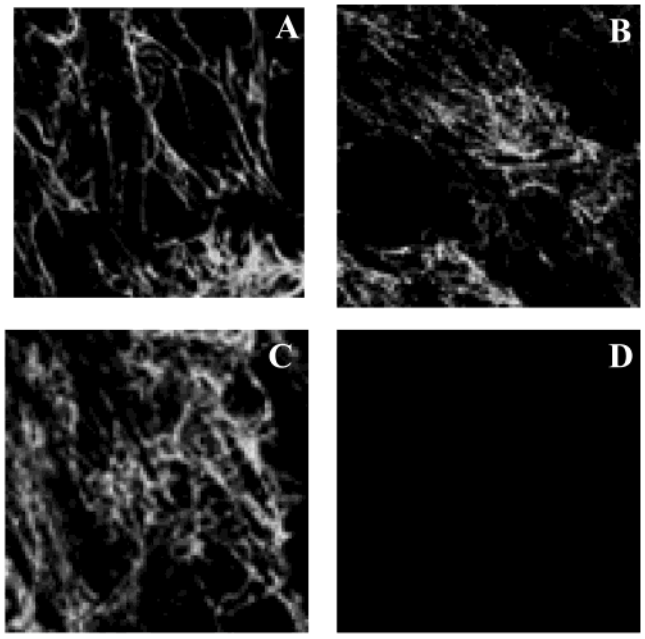

FIGURE 7: Immunofluorescent staining of Fg incorporated into the matrix produced by fibroblasts. WI38 fibroblasts were cultured for 72 h, and then soluble plasma Fg was added. During the next 24 h, Fg was converted to fibrin in the presence of endogenous procoagulant activity, and fibrin became associated with the extracellular matrix produced by fibroblasts. Cells were fixed, and then stained with the following antibodies: (A) mAb 8A11 against fibronectin (5 μg/mL); (B) mAb 2G5 against Fg/fibrin (5 μg/mL); and (C) mAb 4-2 (2 μg/mL). (D) Cells were grown without Fg, and then mAb 4-2 and a secondary antibody were added (control staining).

Fg leaks through the endothelial layer during the inflammatory response and is deposited into the extracellular matrix as fibrin after activation by thrombin (*14*) or in a proteolytically unmodified form (*6*). We have tested whether the epitope for mAb 4-2 is exposed in Fg incorporated in the extracellular matrix. Accordingly, WI38 human lung fibroblasts, which are known to elaborate the extensive extracellular matrix, were cultured to confluence, and then soluble Fg was overlaid onto the cell layer and cells were incubated for extra 24 h. Since no inhibitors of coagulation were added, Fg was converted to a fibrin clot. Fibrin-specific α and β chains were demonstrated by SDS−PAGE of reduced samples (not shown). Immunofluorescent staining of cells was performed using Mab 4-2, in parallel with mAb 8A11 specific for fibronectin and mAb 2G5 which recognizes the epitope γ373−385 in Fg and fibrin (*38*). The pattern of staining characteristic for fibronectin fibrils around and beneath the cells was verified using anti-fibronectin mAb (Figure 7A). Co-culturing of Fg with fibroblasts resulted in deposition of Fg/fibrin into the matrix. Binding of Fg to this endogeneously produced matrix was detected by staining with mAb 2G5 (Figure 7B). The similar fibrillar pattern of staining was also detected using mAb 4-2, suggesting that association of Fg/fibrin with the extracellular matrix resulted in unmasking of the epitope at γ392−400 (Figure 7C).

DISCUSSION

The present study was undertaken to resolve the differential recognition by integrin $\alpha_M\beta_2$ of a soluble form of the Fg molecule from its immobilized form. We show that

the $\alpha_M\beta_2$-binding site in the γC-domain of soluble intact Fg is cryptic and characterize the conformational alterations that evoke its unmasking.

Several observations are consistent with the lack of exposure of the $\alpha_M\beta_2$-binding site in intact Fg. Soluble Fg was a poor inhibitor of neutrophil adhesion to immobilized Fg ligands. Also, the interaction of soluble Fg with the $\alpha_M\beta_2$-transfected HEK 293 cells was not detected, and intact Fg did not inhibit adhesion of these cells to immobilized Fg derivatives. Furthermore, no interaction was observed with the D_{100} fragment which contains the binding site for $\alpha_M\beta_2$ and preserves a conformation inherent to intact Fg in solution. The D_{100} fragment did not inhibit adhesion of the $\alpha_M\beta_2$-bearing cells, including fMLP- and PMA-activated neutrophils. In addition, D_{100} bound poorly to the recombinant α_MI-domain, a recognition domain within $\alpha_M\beta_2$ for Fg (*39*).

Two processes which resulted in unmasking of the $\alpha_M\beta_2$-binding site in Fg and the D_{100} fragment have been identified: (1) immobilization of Fg or D_{100} onto a plastic surface in vitro was associated with extensive exposure of the $\alpha_M\beta_2$-binding site as evidenced by efficient adhesion of neutrophils and the $\alpha_M\beta_2$-expressing HEK 293 cells. Also, we have previously demonstrated that Fg and D_{100}, spontaneously adsorbed on the surface of biomaterial implants in an animal model, mediated phagocyte accumulation (*40*), consistent with an idea that deposits of fibrinogen in vivo are able to support $\alpha_M\beta_2$-mediated leukocyte adhesion; (2) proteolysis of the D_{100} fragment by plasmin generated fragments with properties of competent inhibitors of adhesion of neutrophils and the $\alpha_M\beta_2$-expressing HEK 293 cells, and also increased the binding of these fragments to the recombinant α_MI-domain.

Previous studies demonstrated that the $\alpha_M\beta_2$-binding site in the D fragment resides in the γC-domain and that the sequence γ383−395 (P2-C) may be the major recognition site (*19*)[2]. We found that P2-C is available for interaction with the anti-P2-C-specific mAb 4-2 only in the immobilized Fg and D_{100}. The P2-C sequence is not exposed in soluble Fg and D_{100} as judged by the fact that these proteins are not able to compete with immobilized D_{100} for mAb binding. Proteolysis of D_{100} by plasmin and MMP-3 resulted in enhanced exposure of the P2-C epitope since the D_{98}, D_{80}, and D_s fragments were potent inhibitors of binding of the site-specific mAb to the immobilized D_{100}. Thus, the lack of inhibition of cell adhesion by soluble Fg and D_{100} correlates with the lack of immunoreactivity with anti-P2-C mAb. And vice versa, the ability of D_{98} to inhibit $\alpha_M\beta_2$-mediated adhesion coincides with the immunoreactivity of this fragment with the mAb. The correlation between the inhibitory activity of D_{98} versus D_{100} in the cell adhesion assay and the state of exposure of P2-C in D_{98} and D_{100} further implicates P2-C as the $\alpha_M\beta_2$-binding site in γC.

We propose that immobilization of Fg or D_{100} on a surface (whether it be the plastic or live extracellular matrix) induces a conformational transition that involves changes in the position of the extreme COOH-terminal part of the γC-domain (γ143−411). This supposition is based on the observation that the cleavage of the COOH-terminal part of the γC-domain in the D_{100} fragment by plasmin generates fragments with the ability to inhibit adhesion of neutrophils and the $\alpha_M\beta_2$-expressing cells. In addition, the higher extent of binding of D_{98} to the recombinant α_MI-domain and to the α_MI-domain recognition peptide Glu^{253}−Arg^{261} compared to that of D_{100} is also consistent with the interpretation that the removal of the COOH-terminus in γC unmasks the $\alpha_M\beta_2$-binding site.

The cleavage site in the γ-chain of the D-domain produced by plasmin was previously identified as γLys^{406} (*36*, *41*). The cleavage sites at γAla^{405} and at γGlu^{396} in the D3 fragment corresponding to our D_{80} were also reported (*41*, *42*). Matrix metalloproteinase stromelysin (MMP-3) degrades Fg, cross-linked fibrin, and the DD fragment at γGly^{404}−Ala^{405} (*37*). We demonstrate that MMP-3 also cleaved D_{100} probably at the same position (Figure 4). Thus, the removal of the small COOH-terminal peptides γ405/406−411 and/or γ397−411 from D_{100} resulted in unmasking of the $\alpha_M\beta_2$-binding site.

A higher immunoreactivity of the D_{80} fragment with anti-P2-C mAb 4-2 as compared to that of D_{98} suggests that the P2-C site is more accessible in D_{80}. Recent data revealed that in addition to the γ-chain remnant γ86−302, the D_{80} fragment contains the γ374−405 (or γ374−396) segment which remains inserted as a structural β strand into the central sheet of the γC-domain similar to that in intact γC (*41*). Thus, the presence of γ374−405/396 should provide the basis for the immunoreactivity of D_{80} with mAb 4-2. Indeed, D_{80} reacted with mAb 4-2 in ELISA (not shown). The cleavage at γ373−374 might facilitate the access of the mAb to the epitope. In addition, we and others (*43*) have found that a population of D_{80} molecules had the cleavage(s) at γ192. The observed cleavage occurs in the NH_2-terminal part of the β strand γ190−198 and resides in immediate proximity to the P2-C sequence in the three-dimensional structure of γC (*16*, *17*) (Figure 8, γC). Therefore, it is possible that this internal cleavage could destabilize the association between the subdomains in γC, thus resulting in better accessibility of the P2-C epitope for mAb.

Taken together, our data demonstrate that the C-terminus in the γC-domain may regulate the accessibility to the P2-C region (Figure 8, γC-domain). We speculate that in intact soluble Fg and D_{100}, the COOH-terminal tail may shield this region and limit access to $\alpha_M\beta_2$ and antibodies. In the crystal structure of the γC-domain (*16*, *17*) (Figure 8, γC), the position of γ392−402 was not solved definitively since it was observed in several conformations. The location of the remaining part of the C-terminus beyond γ402 is not clear because it was missing in the crystals due to proteolysis. However, although the overall conformation of the C-terminus in γC is not known, crystallographic, NMR, and electron microscopy analyses indicated that it may be a highly flexible structure (*16*, *44*−*47*). Speculatively, the C-terminus can fold back and assume a conformation in which it masks P2-C (Figure 8A). The conformational flexibility of this "tail" may allow unfolding of this region in γC upon immobilization of Fg and D_{100} onto a plastic surface or in the extracellular matrix, and unmasking of P2-C (Figure 8B). Furthermore, clipping of the C-terminus by proteases should also remove a shield (Figure 8C). Indirect evidence that the C-terminus may fold back is provided by the three-dimensional structure of the γ-chain peptide γ398−411 crystallized as a complex with two different carrier proteins (*44*, *48*). In these structures, a reproducible kink at γHis^{401} and γLeu^{402} and a turn of the remaining segment were observed. In addition, other data supporting the idea

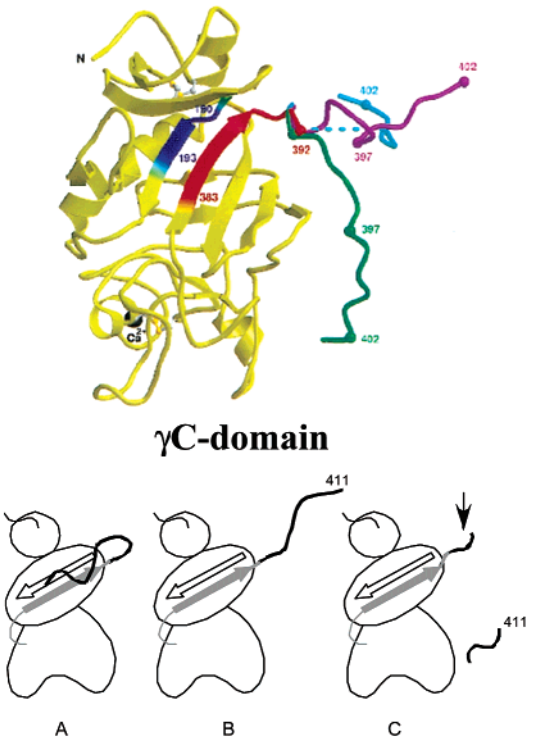

FIGURE 8: Conformational states of the γC-domain regulate availability of P2-C, a putative site for $\alpha_M\beta_2$. The ribbon model of the γC-domain (γ144−402) was drawn according to its crystal structures, PDB identifiers 1fib, 1fic, and 1fid (*16*), using the computer programs BobScript and Raster 3D (*66*, *67*). The γ383−395 (P2-C) region is colored in red. The numbers indicate the position of selected residues in P2-C. The C-terminal region (beyond residue Leu392) is shown in three different conformations as found in different crystal forms of γC (*16*). (A) Schematic representation of the γC-domain in hypothetical "closed" conformation which may exist in intact soluble Fg and the D_{100} fragment. In this conformation, the P2-C sequence is not exposed on the surface of the γC-domain due to the positioning of the γC-terminal tail which is folded back and masks these sequences. (B) Immobilization of Fg or D_{100} onto the surface or deposition into the extracellular matrix induces unmasking of the P2-C region as a result of unfolding and shifting of the C-terminal tail. (C) Proteolytic cleavage of the extreme COOH-terminus of the γ-chain by plasmin, MMP-3, or other proteases perturbs the conformational integrity of the γC-domain and, thus, "unlocks" the putative $\alpha_M\beta_2$-binding site.

that the γC-termini in Fg are oriented toward the center of the molecule were also obtained (*47*). The extension of this hypothesis is that the folded C-terminal "tail" should interact with the core of the γC-domain and stabilize it in the "closed" conformation. The conformational transitions between "open" and "closed" states were observed in other adhesive proteins (*49*, *50*) and in Fg itself (*51*). In this regard, the crystal structure and electron microscopy provided evidence that the C-terminal parts of the Aα-chain in Fg make a turn in the middle of the molecule to fold back toward the central E-domain such that several functional sites become shielded (*17*, *51*). These sites are unmasked upon transformation of fibrinogen to fibrin and by degradation of the molecule. Another mechanism by which the conformation of the C-terminal part of γC can be altered has recently been proposed. Yakovlev et al. (*41*) have put forward a hypothesis according to which the γ381−390 structural β strand could be "pulled-out" from the framework of γC. The γ381−390 sequence overlaps with P2-C and, thus, this process could potentially result in the exposure of P2-C. Further studies will be required to elucidate the nature of conformational alterations in this part of γC.

The three-dimensional structure of the DD fragment, which models the end-to-end association of the γC-domains in the joined D-domains in fibrin, suggests that the C-terminal ends of two γC should come into close proximity to accommodate intermolecular cross-links by Factor XIII (*17*). Although the positions of the cross-linking sites at γGln^{398} and γLys^{406} are not clear in the DD crystal structure, it is obvious that the reciprocally linked C-terminal tails do not mask the P2-C epitope [see Figure 7 in (*34*)]. This is consistent with the interaction of the DD-fragment with the anti-P2-C mAb in our experiments. Furthermore, P2-C is available in fibrin deposited into the extracellular matrix produced by fibroblasts as evidenced by immunofluorescent staining with mAb 4-2 (Figure 7).

The finding that the binding site for $\alpha_M\beta_2$ in Fg is cryptic adds this integrin−ligand pair to the list of known integrin−ligand systems in which molecular recognition is regulated by a conformational alteration of the ligand. Previous data demonstrated that RGD adhesive signals are cryptic or poorly exposed in several integrin ligands, including collagen (*52*, *53*), fibrinogen (*54*), vitronectin (*55*), fibronectin (*30*), tenascin (*56*), laminin (*57*), and thrombospondin (*58*). Although the RGD-containing domains in these proteins were shown to become exposed by different events, unmasking by proteolysis, by immobilization on the surface, and by multimerization are the most common mechanisms. Other adhesive sequences, for example, LDV in the IIICS-1 segment of fibronectin (*59*) which is recognized by $\alpha_4\beta_1$, and adhesive sequences in osteopontin (*60*) and in laminin (*61*) recognized by $\alpha_9\beta_1$ and by $\alpha_6\beta_1$, respectively, are also cryptic in intact molecules and become unmasked by specific proteolytic events. However, while the augmented adhesive activities of the extracellular matrix proteins as a result of conformational alterations were extensively documented, the present study is the first to identify the molecular mechanism responsible for unmasking of the cryptic adhesive site. Thus, we conclude that productive integrin−ligand interactions not only involve well-documented agonist-induced conformational changes in integrins (*62*, *63*) but also require ligand "activation" as well (*64*, *65*).

ACKNOWLEDGMENT

We thank Dr. E. Plow for support during the early stages of this work. We thank Dr. H. Nagase for a generous gift of MMP-3, Dr. G. Matsueda for providing mAb 4A5, Dr. K. Bialkowska for assistance with microscopy, and Tim Burke for valuable comments on the manuscript.

REFERENCES

1. Wu, X., Helfrich, M. H., Horton, M. A., Feigen, L. P., and Lefkowith, J. B. (1994) *J. Clin. Invest. 94*, 928−936.
2. McRitchie, D. I., Girotti, M. J., Glynn, M. F. X., Goldberg, J. M., and Rotstein, O. D. (1991) *J. Lab. Clin. Med. 118*, 48−55.
3. Busso, N., Peclat, V., Van Ness, K., Kolodziesczyk, E., Degen, J., Bugge, T., and So, A. (1998) *J. Clin. Invest. 102*, 41−50.
4. Tang, L., and Eaton, J. W. (1993) *J. Exp. Med. 178*, 2147−2156.
5. Colvin, R. B., Mosesson, M. W., and Dvorak, H. F. (1979) *J. Clin. Invest. 63*, 1302−1306.
6. Bini, A., Fenoglio, J. J., Jr., Mesa-Tejada, R., Kudryk, B., and Kaplan, K. L. (1989) *Arteriosclerosis 9*, 109−121.

7. Valenzuela, R., Shainoff, J. R., DiBello, P. M., Urbanic, D. A., Anderson, J. M., Matsueda, G. R., and Kudryk, B. J. (1992) *Am. J. Pathol. 141*, 861−880.
8. Kuijper, P. H. M., Torres, G., Lammers, J.-W. J., Sixma, J. J., Koenderman, L., and Zwaginga, J. J. (1997) *Blood 89*, 166−175.
9. Massberg, S., Enders, G., de Melo Matos, F. C., Tomic, L. I. D., Leiderer, R., Eisenmenger, S., Messmer, K., and Krombach, F. (1999) *Blood 94*, 3829−3838.
10. Altieri, D. C., Mannucci, P. M., and Capitanio, A. M. (1986) *J. Clin. Invest. 78*, 968−976.
11. Altieri, D. C., Bader, R., Mannucci, P. M., and Edgington, T. S. (1988) *J. Cell Biol. 107*, 1893−1900.
12. Lu, H., Smith, C. W., Perrard, J., Bullard, D., Tang, L., Entman, M. L., Beaudet, A. L., and Ballantyne, C. M. (1997) *J. Clin. Invest. 99*, 1340−1350.
13. Guadiz, G., Sporn, L. A., and Simpson-Haidaris, P. J. (1997) *Blood 90*, 2644−2653.
14. Dvorak, H. F., Senger, D. R., Dvorak, A. M., Harvey, V. S., and McDonagh, J. (1985) *Science 227*, 1059−1061.
15. Medved, L., Litvinovich, S., Ugarova, T., Matsuka, Y., and Ingham, K. (1997) *Biochemistry 36*, 4685−4693.
16. Yee, V. C., Pratt, K. P., Cote, H. C. F., LeTrong, I., Chung, D. W., Davie, E. W., Stenkamp, R. E., and Teller, D. C. (1997) *Structure 5*, 125−138.
17. Spraggon, G., Everse, S. J., and Doolittle, R. F. (1997) *Nature 389*, 455−462.
18. Altieri, D. C., Plescia, J., and Plow, E. F. (1993) *J. Biol. Chem. 268*, 1847−1853.
19. Ugarova, T. P., Solovjov, D. A., Zhang, L., Loukinov, D. I., Yee, V. C., Medved, L. V., and Plow, E. F. (1998) *J. Biol. Chem. 273*, 22519−22527.
20. Forsyth, C. B., Solovjov, D. A., Ugarova, T. P., and Plow, E. F. (2001) *J. Exp. Med. 193*, 1123−1133.
21. Yakubenko, V. P., Solovjov, D. A., Zhang, L., Yee, V. C., Plow, E. F., and Ugarova, T. P. (2001) *J. Biol. Chem. 275*, 13995−14003.
22. Gustafson, E. J., Lukasiewicz, H., Wachtfogel, Y. T., Norton, K. J., Schmaier, A. H., Niewiarowski, S., and Colman, R. W. (1989) *J. Cell Biol. 109*, 377−387.
23. Wright, S. D., Weitz, J. I., Huang, A. J., Levin, S. M., Silverstein, S. C., and Loike, J. D. (1988) *Proc. Natl. Acad. Sci. U.S.A. 85*, 7734−7738.
24. Loike, J. D., Sodeik, B., Cao, L., Leucona, S., Weitz, J. I., Detmers, P. A., Wright, S. D., and Silverstein, S. C. (1991) *Proc. Natl. Acad. Sci. U.S.A. 88*, 1044−1048.
25. Doolittle, R. F., Schubert, D., and Schwartz, S. A. (1967) *Arch. Biochem. Biophys. 118*, 456−467.
26. Ugarova, T. P., and Budzynski, A. Z. (1992) *J. Biol. Chem. 267*, 13687−13693.
27. Olexa, S. A., and Budzynski, A. Z. (1979) *Biochemistry 18*, 991−995.
28. Zhang, L., and Plow, E. F. (1996) *J. Biol. Chem. 271*, 18211−18216.
29. Moskowitz, K. A., Kudryk, B., and Coller, B. S. (1998) *Thromb. Haemostasis 79*, 824−831.
30. Ugarova, T. P., Zamarron, C., Veklich, Y., Bowditch, R. D., Ginsberg, M. H., Weisel, J. W., and Plow, E. F. (1995) *Biochemistry 34*, 4457−4466.
31. Zamarron, C., Ginsberg, M. H., and Plow, E. F. (1991) *J. Biol. Chem. 266*, 16193−16199.
32. Matsueda, G. R., and Bernatowicz, M. S. (1988) in *Fibrinogen 3—Biochemistry, Biological Functions, Gene Regulation and Expression* (Mosesson, M. W., Amrani, D., Siebenlist, K. R., and DiOrio, P., Eds.) pp 133−136, Elsevier Science Publishers B. V., Amsterdam.
33. Lishko, V. K., Yakubenko, V. P., Hertzberg, K. M., Grieninger, G., and Ugarova, T. P. (2001) *Blood 98*, 2448−2455.
34. Ugarova, T. P., and Yakubenko, V. P. (2001) *Ann. N.Y. Acad. Sci. 936*, 368−386.
35. Collen, D., Kudryk, B., Hessel, B., and Blomback, B. (1975) *J. Biol. Chem. 250*, 5808−5817.
36. Varadi, A., and Scheraga, H. A. (1986) *Biochemistry 25*, 519−528.
37. Bini, A., Itoh, Y., Kudryk, B. J., and Nagase, H. (1996) *Biochemistry 35*, 13056−13063.
38. Zamarron, C., Ginsberg, M. H., and Plow, E. F. (1990) *Thromb. Haemostasis 64*, 41−46.
39. Diamond, M. S., Garcia-Aguilar, J., Bickford, J. K., Corbí, A. L., and Springer, T. A. (1993) *J. Cell Biol. 120*, 1031−1043.
40. Tang, L., Ugarova, T. P., Plow, E. F., and Eaton, J. W. (1996) *J. Clin. Invest. 97*, 1329−1334.
41. Yakovlev, S. L. S., Loukinov, D. I., and Medved, L. (2000) *Biochemistry 39*, 15721−15729.
42. Southan, C., Thompson, E., Panico, M., Etienne, T., Morris, H. R., and Lane, D. A. (1985) *J. Biol. Chem. 260*, 13095−13101.
43. Hormann, H., and Henschen, A. (1979) *Thromb. Haemostasis 41*, 691−694.
44. Ware, S., Donahue, J., Hawiger, J., and Anderson, W. F. (1999) *Protein Sci. 8*, 2663−2671.
45. Blumenstein, M., Matsudeda, G. R., Timmons, R., and Hawiger, J. (1992) *Biochemistry 31*, 10692−10698.
46. Mayo, K. H., Fan, F., Beavers, M. P., Eckardt, A., Keane, P., Hoekstra, W. J., and Andrade-Gordon, P. (1996) *FEBS Lett. 378*, 79−82.
47. Mosesson, M. W., Siebenlist, K. R., Meh, D. A., Wall, J. S., and Hainfeld, J. F. (2001) *Proc. Natl. Acad. Sci. U.S.A. 95*, 10511−10516.
48. Donahue, J. P., Patel, H., Anderson, W. F., and Hawiger, J. (1994) *Proc. Natl. Acad. Sci. U.S.A. 91*, 12178−12182.
49. Erickson, H. P., and Carrell, N. A. (1983) *J. Biol. Chem. 258*, 14539−14544.
50. Siedlecki, C. A., Lestini, B. J., Kottke-Marchant, K., Eppell, S. J., Wilson, D. L., and Marchant, R. E. (1996) *Blood 88*, 2939−2950.
51. Veklich, Y. I., Gorkun, O. V., Medved, L. V., Nieuwenhuizen, W., and Weisel, J. W. (1993) *J. Biol. Chem. 268*, 13577−13585.
52. Davis, G. E. (1992) *Exp. Cell Res. 200*, 242−252.
53. Pfaff, M., Aumailley, M., Specks, U., Knolle, J., Zerwes, H.-G., and Timpl, R. (1993) *Exp. Cell Res. 206*, 167−176.
54. Ugarova, T. P., Budzynski, A. Z., Shattil, S. J., Ruggeri, Z. M., Ginsberg, M. H., and Plow, E. F. (1993) *J. Biol. Chem. 268*, 21080−21087.
55. Seiffert, D., and Smith, J. W. (1997) *J. Biol. Chem. 272*, 13705−13710.
56. Denda, S., Muller, U., Crossin, K. L., Erickson, H. P., and Reichardt, L. F. (1998) *Biochemistry 37*, 5464−5474.
57. Aumailley, M., Gerl, M., Sonnenberg, A., Deutzmann, R., and Timpl, R. (1990) *FEBS Lett. 12*, 82−86.
58. Hotchkiss, K. A., Mattias, L. J., and Hogg, P. J. (1998) *Biochim. Biophys. Acta 1388*, 478−488.
59. Ugarova, T., Ljubimov, A. V., Deng, L., and Plow, E. F. (1996) *Biochemistry 35*, 10913−10921.
60. Smith, L. L., Cheung, H.-K., Ling, L. E., Chen, J., Sheppard, D., Pytela, R., and Giachelli, C. M. (1996) *J. Biol. Chem. 271*, 28485−28491.
61. Giannelli, G., Falk-Marzillier, J., Schiraldi, O., Stetler-Stevenson, W. G., and Quaranta, V. (1997) *Science 277*, 225−228.
62. Diamond, M. S., and Springer, T. A. (1994) *Curr. Biol. 4*, 506−517.
63. Humphries, M. J. (2000) *Biochem. Soc. Trans. 28*, 311−340.
64. Ugarova, T. P., Agbanyo, F. R., and Plow, E. F. (1995) *Thromb. Haemostasis 74*, 253−257.
65. Davis, G. E., Bayless, K. J., Davis, M. J., and Meininger, G. A. (2000) *Am. J. Pathol. 156*, 1489−1498.
66. Esnouf, R. M. (1997) *J. Mol. Graph. 15*, 133−138.
67. Merritt, E. A., and Murphy, M. E. P. (1994) *Acta Crystallogr. D50*, 869−873.

BI026324C